Taylor & Francis
Taylor & Francis Group

Topological point defects in nematic liquid crystals

M. KLEMAN*† and O. D. LAVRENTOVICH‡

†Institut de Minéralogie et de Physique des Milieux Condensés
(CNRS UMR 7590), Université Pierre-et-Marie-Curie, Campus Boucicaut,
140 rue de Lourmel, 75015 Paris, France
‡Chemical Physics Interdisciplinary Program and Liquid Crystal Institute,
Kent State University, Kent, Ohio, USA

Point defects in nematics, also called hedgehogs, are topological entities that have no equivalent in ordered atomic solids, despite the homonymy. They have been the subject of intense experimental and, above all, theoretical (analytical and computational) investigations in the last thirty years. They are present in bulk specimens and at the specimen boundaries. This review article stresses the importance of the core structure of the defect, the possibility of it splitting into a disclination loop, and boundary conditions, as well as taking stock of the recent advances on point defects in nematic colloidal suspensions. An important topic is the formation of strings between opposite hedgehogs (radial and hyperbolic), and their role in the dynamic properties of nematics.

1. Introduction

A nematic liquid crystal is an anisotropic fluid formed by rod-like or disk-like molecules that tend to be parallel to a common direction, the director, denoted $\mathbf{n}$ ($\mathbf{n}^2 = 1$). The directions $\mathbf{n}$ and $-\mathbf{n}$ are physically equivalent: $\mathbf{n} \equiv -\mathbf{n}$. There is no long-range translational order in the system and thus nematics are fluid and very sensitive to an external field, which explains why they became a key technological material in applications such as informational displays. Nematic liquid crystals are in the focus of intensive interdisciplinary studies also because they represent a well-defined soft matter system with a rich variety of supramolecular structures, most notably those corresponding to the so-called topological defects. A topological defect is a configuration of the order parameter that cannot be transformed continuously into a uniform state. They can occur during symmetry-breaking phase transitions, under an external field, or simply be a necessary element of an equilibrium state. For example, in a sufficiently large spherical nematic droplet

*Corresponding author. Email: maurice.kleman@mines.org

with perpendicular alignment of molecules at the surface, the director field forms a radial-like configuration with a point defect at the centre, in order to reach an equilibrium state. This point defect in the director configuration is of a completely different nature compared to point defects, such as vacancies and interstitials, in solid crystals [1]; its topological nature means that the distortions of the order parameter around the "point" extend throughout the entire system.

The singular points of a vector field (cols, nœuds, foyers, etc.) were classified by Poincaré [2], by using the tools of the theory of ordinary differential equations; Nabarro [3] was the first to notice that Poincaré's method can be applied, with the purpose of classifying point defects, to spins in a ferromagnet and directors in a nematic insofar as the sample does not show circuits along which **n** is reversed.

The topological classification of defects, on the other hand, relies on the topological properties of the order parameter space. It does not give a classification as detailed as the vector field one, but its principles can be extended to any ordered medium and to defects of any dimensionality [4, 5]. The scalar order parameter, $S(T)$, of a uniaxial nematic is the thermal mean, $\frac{1}{2} <(3\cos^2\theta - 1)>$, of the orientation of the molecules about the director. More precisely, the order parameter (OP) is a traceless tensor, $Q_{ij} = S(T)(n_i n_j - \frac{1}{3}\delta_{ij})$. The OP space is the space of all the realizations of the OP. In the case of a uniaxial nematic, a sphere of unit radius represents adequately all the directions of **n**; the OP space is therefore a half sphere, namely the projective plane, denoted P_2 (see Hilbert and Cohn-Vossen [6]). Topological defects of various dimensionalities, d, in ordered media are classified by the homotopy groups $\Pi_n(V)$, $n = D - d - 1$, where D is the space dimension; in a 3D nematic, $V = P_2$, $n = 1$ stands for line defects (disclinations), $n = 2$ for point defects. The topological charge (an invariant) carried by a point defect can be calculated by the relation [7]

$$4\pi N = \iint \varepsilon_{ijk}\varepsilon_{pqr}n_{q,j}n_{r,k}n_p dS_i \tag{1}$$

where the integration is performed on a sphere-like surface surrounding the singular point. N is an integer; $\Pi_2(V) = Z$. Point defects ($N = \pm 1$), the only ones ever observed experimentally, are called hedgehogs. As equation (1) is odd in the director components and $\mathbf{n} \equiv -\mathbf{n}$, the same point defect can be assigned opposite charges: also, the charge can be drawn opposite by a circumnavigation of the point defect around a disclination line of strength $k = \pm\frac{1}{2}$ (about which the director changes sign) [8]. It is usual to assign the value $N = +1$ to a radial hedgehog and $N = -1$ to a hyperbolic hedgehog (see figure 1). Nabarro [9] was probably the first to show a keen interest in the topology of defects in a nematic by noticing that the Euler–Poincaré characteristic of a sphere [5] measures the total strength of the disclinations piercing the boundary of a nematic droplet, if the boundary conditions are such that the director is everywhere parallel to the droplet surface ($\Sigma_i k_i = 2$).

The free energy density associated with the changes of the tensor order parameter in the vicinity of the nematic–isotropic phase transition is of the Landau–De Gennes form:

$$f_{LdG} = \frac{1}{2}a(T,p)\mathrm{tr}Q^2 - \frac{1}{3}b\mathrm{tr}Q^3 + \frac{1}{4}c(\mathrm{tr}Q^2)^2. \tag{2}$$
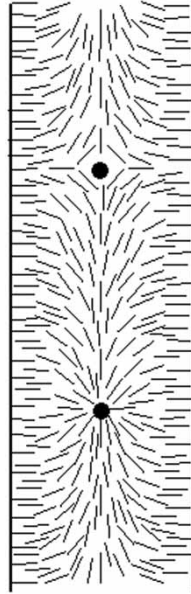
Figure 1. Capillary tube with homeotropic, i.e. normal, boundary conditions: meridian section. The director is in the meridian plane. Point defects $N=+1$ (radial hedgehog) and $N=-1$ (hyperbolic hedgehog).

When the scalar order parameter does not change much, which is true for director deformations over the scales much larger than the molecular size, then the free energy density of the elastic director distortion is written as the Frank–Oseen expression

$$f_{Fr} = \frac{1}{2}K_1(\mathrm{div}\,\mathbf{n})^2 + \frac{1}{2}K_2(\mathbf{n} \times \mathrm{curl}\,\mathbf{n})^2 + \frac{1}{2}K_3(\mathbf{n} \times \mathrm{curl}\,\mathbf{n})^2 - K_{24}\mathrm{div}\,(\mathbf{n}\,\mathrm{div}\,\mathbf{n} + \mathbf{n} \times \mathrm{curl}\,\mathbf{n})$$

(3)

with Frank elastic constants of splay (K_1), twist (K_2), bend (K_3), and saddle-splay (K_{24}).

Melzer and Nabarro [10, 11] also made very early observations of hedgehogs in capillaries. In fact, there have been very few detailed experimental investigations of hedgehogs in the course of time since their appearance in the realm of nematics compared to the flourish of theoretical studies, the latter encouraged by the development of computer methods. On the other hand, theory and experiment seem to go hand in hand for point defects in colloidal suspensions in nematics, where an air bubble (which acts as a positive $N=+1$ point defect) or a droplet or a particle that compensate a negative $N=-1$ point defect in their vicinity [12], can form a stable dipole.

This paper presents a brief review of bulk point defects (hedgehogs) and surface singular points, often called boojums (the name is due to Lewis Carroll and has been adopted frenetically by the superfluid and liquid crystal communities thanks to Mermin).

2. Bulk and surface singular points

2.1. *Static observations*

Defects usually appear in the bulk of a sample by symmetry breaking, at the isotropic–nematic transition, T_{IN}, either by a thermal quench or a slow transition; pressure quench has also been employed. One expects to obtain in this way a random array of defects of various dimensionalities: point defects, disclination lines, and configurations or solitons (non-singular topological defects) [4]. The final defect distribution depends on the time of annealing and on the boundary conditions, i.e. on the anchoring conditions at the boundaries of the sample, like those induced by a physical or chemical surface treatment; this forces the orientation of the molecule.

We are interested in point defects. A remarkable experimental result is that their occurrence in the bulk just after quench (independently of the boundary conditions) is a rather rare, if ever observed, event [13]. An interesting (and subtle) explanation has been given of this phenomenon [14]. The topological charge, N of equation (1), measures twice the number of times that P_2 is covered by the order parameter (the director); this is a rather difficult geometric requirement to be obeyed by the correlated nematic domains which appear randomly about some point of the sample at the transition. The probability of this event can be calculated [14]. The idea follows the lines of the celebrated Kibble mechanism for the generation of cosmic strings (considered as singularity lines) in the early universe [15], which has inspired laboratory experiments on liquid crystals (see, for example, Chuang *et al.* [16]).

Hedgehogs are thus observed in special geometries with specific anchoring conditions, namely in capillaries [10, 11, 17–20], in nematic droplets [21] and in confined parallel samples with hybrid boundary conditions [22, 23]. Our references are not exhaustive. On the other hand, hedgehogs are the rule rather than the exception, in nematic colloidal suspensions (see next section), but this also proceeds from the special anchoring conditions met in such systems.

In capillaries with homeotropic anchoring, the molecules normal to the boundaries force a radial geometry, as pictured in figure 1; one observes that the director 'escapes along the 3rd dimension', i.e. the axis of the capillary, as aptly worded by Meyer [24]. The $k = +1$ disclination forced by the boundary conditions is therefore continuous along its core (or, differently stated, coreless). Observe that the escape is either up or down, with equal probabilities if the normal anchoring is perfect. Thus two types of point defects do appear, of opposite charges $N = \pm 1$. The director configuration can be investigated experimentally by polarized light microscopy; the resulting observations satisfy the expected geometry, at least qualitatively; this experimental method does not allow a large resolution. Therefore the role played by the anisotropy of the elastic moduli, K_1, K_2, and K_3, in the director configuration around the hedgehogs [24, 25] has not yet been satisfactorily tested.

This same anisotropy is also responsible for the configuration of the director about $k = +1$ disclination lines, and also about $k = -1$ lines (see Anisimov and Dzyaloshinskii [26]). Disclination lines can be observed end-on in well-annealed nematic samples formed between two flat glass plates (Schlieren textures, see figure 2). Topology requires that the sum total of the disclination charges
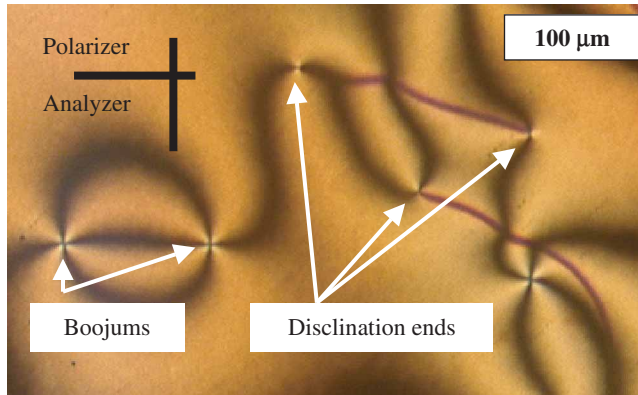
Figure 2. Schlieren texture in a sample with degenerate planar anchoring conditions. The sample is observed between crossed polars. There are two black brushes associated with the $k = \pm\frac{1}{2}$ lines and four brushes (the Maltese cross) associated with the $k = \pm 1$ lines.

vanishes, $\Sigma_i k_i = 0$. One observes $k = \pm\frac{1}{2}$ and $k = \pm 1$ lines. In most experimental cases, in particular SMLCs (small molecule liquid crystals), the escaped geometry is stable with respect to planar singular, i.e. $k = \pm 1$ line geometries, and point defects are present; the situation is more involved in main chain PLCs (polymer liquid crystals) where usually the splay modulus is so large that the escape can be absent in a radial geometry [27]. Thus, apart from a few exceptions, there is ample evidence that the integer lines are coreless and carry point defects, often located outside the sample. Monte Carlo calculations have confirmed these results [28].

The topology of a droplet with homeotropic anchoring is compatible with a radial hedgehog, but its actual presence depends on the anchoring energy, $\sim W\delta^2$ (which measures the excess surface energy necessary to turn the director away from the normal direction by an angle δ; W is called the surface anchoring coefficient), and the droplet size, R. Compare the surface energy, which scales as WR^2 for a uniform director, and the bulk energy, which scales as $(K/R^2)R^3 = KR$ for a radial hedgehog; it is easy to convince oneself that in a droplet of radius R smaller than approximately $R_c = K/W$ the director is uniform, whereas a larger droplet contains a radial hedgehog [4].

In a droplet with planar (degenerate) anchoring, the director field should obey the Euler–Poincaré theorem [6, 9] and, accordingly, must suffer either two singularities with $k = 1$ or one singularity with $k = 2$. The first case (two $k = 1$ singularities) is often met when a nematic droplet is suspended in an isotropic fluid such as glycerol, say [21, 29]; the second one being more specific of biaxial nematics (for the existence of which there appears to be new experimental evidence [30, 31]). Note that in both cases the point defects are essentially surface defects that cannot move inside the nematic bulk because of the boundary conditions. They are thus different from the hedgehogs that can exist both in the bulk and at the surface. Due to this distinction, these surface defects are called boojums [32]; a necessary condition for their formation is that the director field is either tangential or tilted with respect to the surface so that the defect is characterized by an invariant k in addition to N [21].

Finally, hybrid samples: a typical example is when a thin nematic film is spread onto the surface of an isotropic fluid at which the director is oriented tangentially (planar degenerate alignment) whereas the upper boundary is free. Quite often the spontaneous anchoring at the nematic-air interface is homeotropic or tilted. The competition between the two anchoring modes is relaxed by the presence of surface point defects [22, 23].

2.2. *Theory of the static point defect*

In the one-constant approximation (i.e. $K = K_1 = K_2 = K_3$) the geometry of a point defect can be represented near its core by the equations

$$\phi = N\theta_r + \phi_0, \quad \tan\frac{\theta}{2} = \left(\tan\frac{\lambda}{2}\right)^N \tag{4}$$

where θ, ϕ are spherical angles for the director in r; θ_r the polar angle of r in the horizontal plane, λ the angle between the Oz axis and the direction r [18]. It is apparent that $\theta = +\lambda$ for the star-like radial hedgehog, $\theta = -\lambda$ for the hyperbolic hedgehog. The energy does not diverge on the core; one gets, for the radial hedgehog, by integrating the free energy density all over a ball of radius R with a point defect at the centre

$$E_1 = 8\pi KR \tag{5a}$$

and

$$E_{-1} = \frac{1}{3}8\pi KR \tag{5b}$$

for the hyperbolic hedgehog [33].

Of course, there is a physical core, where the nature of the order parameter is modified with respect to the region of 'good' crystal. Let us write for the radial hedgehog the total energy as

$$E_1^{\text{tot}} = 8\pi K(R - r_c) + \gamma r_c^3. \tag{6}$$

Minimizing this expression, one gets

$$r_c = \sqrt{8\pi K/3\gamma}; \quad E_1^{\text{tot}} = 8\pi K\left(R - \frac{2}{3}\sqrt{8\pi K/3\gamma}\right). \tag{7}$$

r_c does not depend on the size, R, of the sample and the energy is not significantly different from E_1, if the core is microscopic compared to R, as expected. Therefore, one can adopt E_1 as a first approximation for the total energy.

To find the minimizer of the integral $\frac{1}{2}\int(\nabla\mathbf{n})^2$ (one-constant approximation) in a given volume $U \subset \mathbf{R}^3$ is a problem relevant to the theory of harmonic maps with defects [34]. An interesting result is that the minimal energy $E_{\cup\{i\}}$ of a set $\cup\{i\}$ of given point defects {i} with $N_i = \pm 1$, such that $\sum N_i = 0$, is given by the expression

$$E_{\cup\{i\}} = 4\pi KL \tag{8}$$

where L is the minimal total length of the dipoles formed by linking point defects of opposite signs two by two. One cannot overestimate the physical importance of this result that stresses the interactions between opposite hedgehogs. These dipoles are indeed visible in Schlieren textures. A somewhat analogous result was obtained by Ostlund [35] and Brinkman and Cladis [36] through a dimensional analysis, but for a unique pair.

Experimental observations show that the real situation is somewhat more complex, even if some results of the simple model above do subsist: (a) K_2 is always small compared to the other moduli; it is then expected that the radial symmetry could be broken by a twist deformation. This phenomenon has been observed for surface defects, boojums in Schlieren textures of lens-shaped droplets [37] and for radial hedgehogs in droplets [29], and studied later for spherical bipolar droplets with pairs of boojums at the poles, both experimentally [21, 38] and theoretically [39, 40]; in relation to these investigations, a radial hedgehog is not a minimizer in a ball with homeotropic conditions, if the Frank constants are anisotropic [41]; (b) as pointed by Press and Arrott [37], the structure of defects is influenced by the splay-cancelling mechanism, according to which the energy of splay deformations along one direction can be reduced by splay in another direction, somewhat similar to the phenomenon of soap films adopting a catenoid shape; (c) it has been suggested by Melzer and Nabarro [10, 11], on the basis of their observations, that point defects might be split into disclination loops, of strength $k=+\frac{1}{2}$ for a radial hedgehog, of strength $k=-\frac{1}{2}$ for a hyperbolic hedgehog (figure 3).

Two theoretical elements have been put forward which complete the present picture of point defects in nematics: (a) the divergence moduli K_{13} and K_{24} can play
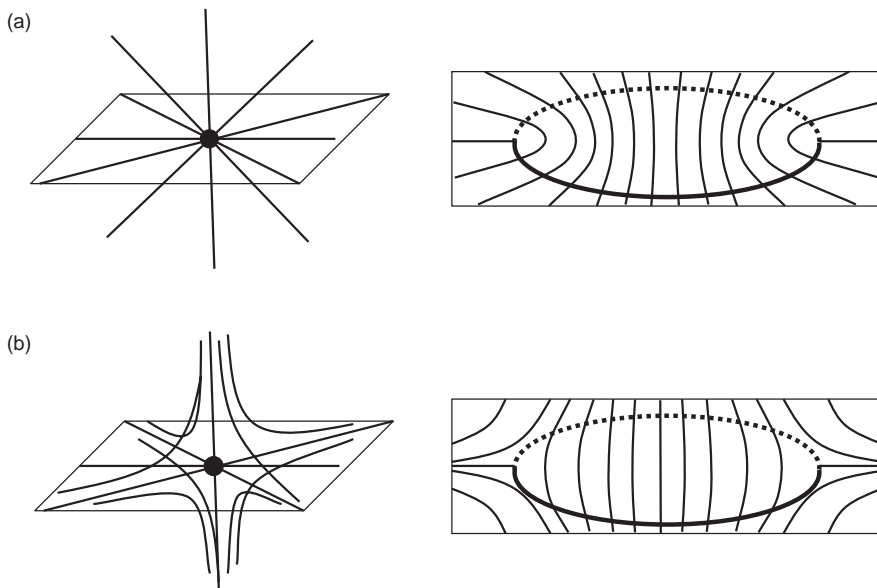

Figure 3. Splitting of point defects into disclination loops: (a) $N=1$ ($\equiv k=\frac{1}{2}$); (b) $N=-1$ ($\equiv k=-\frac{1}{2}$).

a role in the stability of the model, in particular might decide whether the point defect is split, or not, into a disclination loop; (b) the order parameter might change smoothly in the core region, not only in modulus, but also in character. It has indeed been suggested that it might be biaxial [42]. Computer calculations validate this suggestion. We comment on these two points.

The Frank–Oseen elastic theory in the director representation has been used by Mori and Nakanishi [43] and Lavrentovich *et al.* [44] to compare the energies of the hedgehogs and their disclination loop modifications. The divergence elastic term K_{24} is introduced by Lavrentovich *et al.* [44]. Equations (5a) and (5b) become

$$E_{+1}^{\text{tot}} = 8\pi(K - K_{24})(R - r_c) + \gamma r_c^3 \tag{9a}$$

for a radial hedgehog, and

$$E_{-1}^{\text{tot}} = \frac{1}{3} 8\pi(K + K_{24})(R - r_c) + \gamma r_c^3 \tag{9b}$$

for a hyperbolic hedgehog. The transformation to a disclination loop of radius ρ adds in both cases a term of the order of ρK_{24}. It is clear that in the frame of this simplified model the $k = \frac{1}{2}$ loop is forced to expand if $K_{24} < 0$, to shrink if $K_{24} > 0$, the reverse being true for the $k = -\frac{1}{2}$ loop. The radius of the loop stabilizes for a value $\rho \sim \xi \exp -(4K_{24}/K)$, which is microscopic ($\xi$ is the nematic coherence length). By applying the electric field perpendicular to the loop in a nematic material with a positive dielectric anisotropy, one can expand the loop to a larger radius [45]. (See Fukuda and Yokoyama [46] for a recent calculation of the hyperbolic hedgehog in the same vein, but using the full Frank moduli anisotropy).

For the study of the core itself, the Landau–de Gennes theory has been largely employed, allowing a variation of the scalar order parameter. It has been shown by Schopol and Sluckin [47] that spherically symmetric configurations are exact solutions which minimize the Landau-de Gennes free energy, and that the core, whose size is found large compared to ξ, is isotropic. But disclination loops are also solutions. A number of studies [48, 49] have exploited with success the suggestion that the core of a $|k| = \frac{1}{2}$ line is biaxial [42, 50, 51].

Complete models with anisotropic coefficients, divergence elastic terms, Landau expansion in the full free energy, to what has to be added the role of boundary conditions at a finite distance, produce more complicated results (see, for example, Gartland, Jr. and Mkaddem [52, 53] and Kralj *et al.* [54, 55]). Of course, these new developments often require heavy computational methods (see Lavrentovich *et al.* [56]).

2.3. *Interaction and dynamics of defects*

As stated above, radial and hyperbolic hedgehogs couple in 3D uniaxial nematic, by a soliton string in which most of the energy is concentrated (figure 4). For the pair of hedgehogs of opposite topological charge, the director field within the soliton can be written as [57]

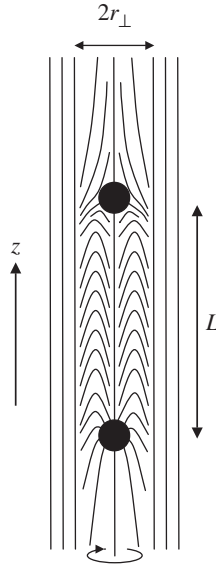$$\mathbf{n} = \left(\frac{x}{r}\sin\theta, \frac{y}{r}\sin\theta, \cos\theta\right),$$

Figure 4. Schematic director configuration of the hedgehog pair connected by a soliton string.

where $\theta = 2 \arctan r_\perp / r$, $r = \sqrt{x^2 + y^2}$, and $r_\perp$ is the soliton radius and z-axis is the axis of rotation symmetry. In an infinite sample, from the point of view of the Frank–Oseen model, there is no mechanism and no typical length to keep r from becoming a zero; when $r_\perp \to 0$, the energy per unit length of the string attains its minimum value $4\pi K$ [57]. As the director gradients diverge at the core for $r_\perp \to 0$, a more refined approach is needed. Penzenstadler and Trebin [48] considered the Landau–de Gennes theory in which the high density of director distortions is relaxed by changing the uniaxial orientational order into the biaxial one, in the spirit of Lyuksyutov's approach to the problem of the singular core of disclinations and point defects [42, 47]. They demonstrated that the soliton can decay into a uniform director structure $\mathbf{n} = const$ by a mechanism of escape to biaxiality [48]. However, the decay might be prevented by the energy barrier separating the uniform state from the soliton state. A stabilization mechanism has been found by Semenov [57], who added a 4th-order gradient term to the standard 2nd order Frank–Oseen functional, $f_{Fr} = (K/2)\nabla \mathbf{n}^2 + K\xi^2 (\nabla \mathbf{n})^2$. This term prescribes the soliton string to be of a (generally macroscopic) fixed radius determined by the separation distance, L, between the point defects located at $z = \pm L/2$ and the nematic coherence length ξ (of the order of a molecular size), namely, $r_\perp(z) \sim \sqrt{\xi L(1 - 4z^2/L^2)}$. The attraction force between the defects acquires a small correction term [57],

$$f = -4\pi K \left(1 + \frac{3}{\sqrt{2}} \frac{\xi}{L} \sqrt{\ln \frac{L}{\xi}}\right).$$

Any realistic liquid crystal sample is bounded; the consideration above then might be applicable only when the characteristic size, R, of the system is much

larger than L. When the two are comparable, the theory should take into account the boundary conditions, namely, the "anchoring" direction and energy associated with the director alignment at the bounding surfaces. In addition to R, the new macroscopic length scale is K/W, usually ranging $0.01\,\mu m$ to $10\,\mu m$. The problem becomes much more complicated and the existing models often offer conflicting views even for the simplest geometry of a bounded sample, such as the circular capillary depicted in figure 1. Semenov's theory [57] and the numerical analysis by Gartland *et al.* [58] predict that the attraction of a pair of points in the capillary can still be described by the expression above but only when L is very short, much shorter than $L^* \sim d_c^{2/3}\xi^{1/3}$ that depends on the capillary diameter d_c; for $L > d_c$, the attractive force decreases exponentially as $\exp(-6.6L/d_c)$, setting the hedgehogs "asymptotically free" and non-interactive at large separations. Qualitatively, the bounding surface sets the director field practically the same on the both sides of each defect core which implies that there is no net force acting on the defect. Guidone Peroli and Virga [59, 60] also predicted an attractive potential, but of a different type: the attractive force varies logarithmically with L at short distances and vanishes at $L \geq 1.1 d_c$. Finally, a model by Vilfan *et al.* [61] predicted that the defects would attract only when $L < 0.1 d_c$ and repel if set at a larger separations. This last model has been inspired by an experimental NMR evidence that in very narrow (submicron) cylindrical cavities, there might exist a (metastable) state with alternating radial and hyperbolic hedgehogs separated by $L \approx d_c$ [62] (see also the numeric simulations in Bradac *et al.* [63]). Although all models dealt with the same basic director geometry, the boundary conditions have been chosen a bit differently, which might explain the discrepancies, according to Holyst and Oswald [64]: the surface anchoring was assumed to be infinitely strong, $W \to \infty$, thus rigidly fixing the director orientation at the boundary [57] was taken as finite by Vilfan *et al.* [61], thus allowing for the (small) director deviations from the anchoring direction at the surface.

Experimentally, the interaction of the topological point defects can be studied in dynamical settings, by studying whether and how the defects of opposite topological charge would attract each other and annihilate. As the first example, consider two point defects in an infinitely large sample, connected by a string of a constant width r whose elastic energy per unit length is $\sim K$. When the two defects approach each other, the director reorientation and thus energy dissipation take place mostly in the region of size $\sim r$; the drag force acting on the defects moving with the closing velocity, $v \sim -dL/dt$, is then $\sim \gamma_1 r v$, where γ_1 is the viscosity coefficient for director reorientations. By equating this force to the elastic force, $\sim K$, one concludes that the two defects should approach each other with a constant velocity; or, equivalently, that the distance between the defects decreases linearly with time:

$$L(t) \propto t_0 - t, \qquad (10)$$

where t_0 denotes the moment of annihilation. Interestingly, when the soliton width tends to zero, $r_\perp \to 0$, as in the case of infinitely large system with two point defects, then the energy dissipation rate should diverge to infinity; as the elastic force remain constant, it means $v \to 0$ [65]. Pismen and Rubinstein [65] interpret this result as an indication that the local reduction of the uniaxial nematic order in the core region

is essential for the defect interaction and dynamics and deduced that the distance changes as

$$L(t) \propto \sqrt{t_0 - t}. \qquad (11)$$

The dynamics obviously change when the potential of interaction changes. For example, if the interaction potential is of a logarithmic type $\sim \ln L/\xi$ (which is the case, for example, of point defects in 2D or straight parallel disclinations in 3D [66]), then the elastic force is $\sim -1/L$ and the drag force is $\sim \gamma_1 v \ln L/\xi$; therefore, the defects move with acceleration and $L(t) \propto \sqrt{t_0 - t}$, or, including the logarithmic correction, $L^2(\ln(L/\xi) + \text{const}) \propto t_0 - t$, still similar to equation (11).

The dependence $L(t) \propto t_0 - t$ for the situation when the defects are indeed connected by an experimentally observable linear soliton of a constant width, over which the director experiences a rotation by 2π (similarly to figure 4, but not axially symmetric) has been confirmed for the pairs of boojums at the surface of the hybrid aligned nematic films [22, 67] and for the defects in freely suspended SmC films [68]. The stability of the soliton requires some "ordering field" [68] (e.g. an in-plane electric field [67] or a film thickness gradient [69]) to confine the director distortions within a region of a constant width. When the solitons do not exist, and the director distortions spread in the entire region between the defects, the dynamics trend changes from equation (10) to equation (11), as observed in the experimental situations [22, 67, 68] above and in the hybrid aligned films of thermotropic nematic polyesters with boojums [23]. Even when the solitons connecting the point exist, one can observe a crossover from $L(t) \propto t_0 - t$ to $L(t) \propto \sqrt{t_0 - t}$ when the separation distance shrinks and becomes smaller than the width of the soliton, at the late stages of annihilation [67].

The experimental situation with the point defects in circular capillaries is even more complex. Both dependencies above have been observed for annihilating pairs of hyperbolic and radial hedgehogs produced by the isotropic-to-nematic quench in circular capillaries with $d_c = 350\,\mu\text{m}$ [20]: $L(t) \propto t_0 - t$ for $L \geq d_c$ and $L(t) \propto \sqrt{t_0 - t}$ for $L \leq d_c$. A similar experiment [70] with $60\,\mu\text{m} \leq d_c \leq 150\,\mu\text{m}$ performed for a similar thermotropic cyanobiphenyl nematic material produced a different result: the sufficiently separated pairs $L \geq d_c$ of hyperbolic and radial hedgehogs at the axis of the capillary did not show any signs of interaction; their separation remained fixed for many hours. Once set in motion by an external perturbation such as temperature gradient along the cylinder, the defects approach each other, first with $L(t) \propto t_0 - t$ when $L \geq d_c$ and with $L(t)$ exponentially vanishing at the final stages of annihilation [70]. This is in contrast to the experiment [20] where the hedgehogs were observed to approach each other even when separated by $L \approx 6d_c$, with a constant velocity, equation (10), which was interpreted as the result of an elastic interaction with a constant force $\sim K$. On the other hand, the experimental technique used by Pargellis *et al.* [20] to produce the defects, namely a fast temperature or pressure quench, might have led to temperature gradients capable of setting the hedgehogs into motion even in the absence of such an interaction. For example, the temperature difference on the two sides of a hedgehog would cause a difference in the Frank elastic constants and thus in the elastic energies of these two regions. Guidone Peroli *et al.* [71] also found $L(t) \propto t_0 - t$ for $L \geq d_c$. However, they interpret

it as the result of the imperfection in the normal alignment at the cylindrical wall [71] rather as the result of any proper elastic interaction between the defects which was taken as non-existent for $L \geq d_c$. To illustrate the point, consider figure 1 and assume that the director at the boundary slightly deviates from the perpendicular orientation, by an angle, φ, say, downwards, so that the director ticks at the right boundary in figure 1 turn from 3 o'clock towards 4 o'clock and the ticks at the left boundary turn from 9 o'clock towards 8 o'clock. Such a deviation might quite naturally be induced by the flow of the nematic fluid during the capillary filling. Then the elastic energy (per unit length) of the configuration that escapes "downwards" (between the two defect cores in figure 1) will be larger than the energy and "upward" escape (outside the defect pair), as the director rotates by $\pi + 2\varphi$ across the capillary in the first case and by $\pi - 2\varphi$ in the second case. The energy of the escaped configuration scales as $\sim K$ (it is independent of d_c [4]) and so does the difference in the elastic energies (per unit length) of the two regions. Therefore, the defects would approach each other to reduce the length of the "overdistorted" region and the dynamics should follow equation (10) [71]. By reversing the sign of φ, the same argument should see the two defects in figure 1 moving in opposite direction: the two would repel each other rather than attract [71]. It might be of interest to verify this feature in experiments by establishing the polarity of the director tilt with respect to the polarity of the hedgehog pair(s).

To conclude, the only relatively well established experimental result for a pair of hedgehogs in circular capillaries is that at short distances, $L \leq d_c$, their dynamics can be described by equation (11) (as also confirmed in numerical simulations with the Lebwohl–Lasher lattice model [72]). What happens at $L \geq d_c$ is not entirely clear. Recently, Holyst and Oswald [64] proposed using a somewhat different geometry, a set of hedgehogs at the singular disclination line that forms near a cylindrical meniscus of a nematic sample in contact with air. Subsequent experiments left the group "certain that ''+1'' and ''−1'' defects attract each other over at short distances and repel at large distances" [73]. Note that all the experiments performed so far reduce to the passive observation of defects locations and their change in time; in the future, it might be useful to add a new experimental technique of a controlled trapping and manipulating the defects with optical tweezers (see, for example Hotta *et al*. [74] and Smalyukh *et al*. [75]).

An important feature of the hedgehog dynamics at short separation distances established by Cladis and Brand [70] is that the radial and hyperbolic hedgehogs move towards each other in the capillary with different velocities; the former moving noticeably faster than the second one, especially near the nematic–smectic transition, where the bend deformations characteristic for the hyperbolic defect become accompanied by a very large elastic constant. The result is most probably related to the backflow effect, i.e. the flow of the nematic fluid caused by director reorientation. Although the backflow effect is of certain importance in any defect dynamics problem, it is extremely difficult to incorporate into the models and is usually neglected. Nevertheless, Blanc *et al*. [76] recently demonstrated that in the similar problem of dynamics of two linear disclinations, the difference in the velocities of the defects of different strength is related to the backflow effect rather than to the elastic anisotropy.

The dynamics of defects has been attracted interest also from the point of view of the phase transition scenarios, not only in liquid crystals and condensed matter, but also in cosmological models (the Kibble model and Zureck model, for example [77]). During the quench from the highly symmetric phase (such as the isotropic fluid) to the lower symmetry phase (a uniaxial nematic, for example), the different pieces of the new phase might acquire different values of the order parameter phase (the director orientation) [4]; when they expand and meet each other, these differences produce topological defects. The quench is then followed by a relaxation process in which the density, N, of defects decreases as the result of their annihilation; for the hedgehogs, the rule should be $N(t) \propto L^{-D}$, in D-dimensional space (see, for example, Toyoki [78] and Wickham [79]). The isotropic–nematic transition has attracted especial interest in this regard [16, 80], mostly because of the (apparent) ease with which the experimental data can be created and collected. The latest theoretical result predicts that in 3D, the hedgehog densities should decay as $N(t) \propto L^{-3} \propto t^{-3/2}$ if there are no other defects such as disclinations. In the experiments by Chuang *et al.* [16], however, the number of hedgehogs has been observed first to increase immediately after the quench, then reach a maximum and quickly decrease, approximately as $N(t) \propto t^{-3}$. These unusual features might be related to the presence of disclinations and to the mutual transformations of hedgehogs and disclination rings. A direct hedgehog–hedgehog annihilation in the 3D nematic bulk without disclination lines involved has been reported to obey equation (11) [81]. The same behaviour, equation (11) with $N(t) \propto L^{-2}$, has been observed by Dierking *et al.* [82] for the annihilation dynamics of umbilical defects in 2D. A single umbilical defect represents a pair of two surface defects, boojums on the opposite sides of the flat cell filled with the nematic of a negative dielectric anisotropy; they appear when a strong electric field is applied to the cell and the director realigns from its original homeotropic orientation. As in the case of pair annihilation in a cylindrical capillary, much more needs to be done before the dynamics of defect tangles in quenched systems with hedgehogs and disclinations can be completely understood. Note that for the clarification of the role of backflow effect the studies of dynamics of boojums and umbilicals might be very productive: the singular (molecular) core that creates problem in many computer simulations does not exist here, as the "cores" of the surface defects and umbilicals are macroscopic.

3. Singular points in nematic colloidal suspensions

Colloids in which the liquid crystal is either a dispersed component [83] or nematic colloids in which the liquid crystal serves as a medium containing droplets of water or solid particles [84, 85], are populated by point defects whenever the surface anchoring at the interfaces is strong enough ($R \gg K/W$). Different boundary conditions (director normal to the interface, tangential, or tilted) lead to two different types of point defects. For example, the equilibrium state of a spherical nematic droplet with normal orientation corresponds to a radial hedgehog (or its topological equivalent such as a ring), while tilted or tangential orientation lead to boojums (surface defects) (figure 5).
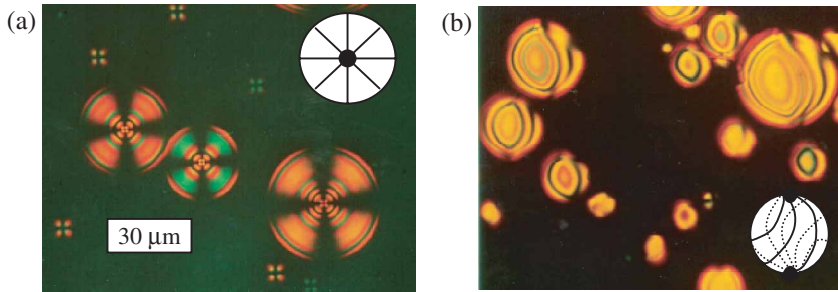
Figure 5. Experimental textures of radial (a) and twisted bipolar nematic droplets (b) viewed between two crossed polarizers.

The topological characteristics of all point defects in a single connected nematic volume must satisfy the restrictions imposed by the Euler–Poincaré and Gauss theorems. For p hedgehogs and q boojums enclosed by a surface of an Euler characteristic, E, the restrictions are [21]

$$\sum_{i=1}^{q+p} N_i = E/2; \quad \sum_{j=1}^{p} k_j = E. \tag{12}$$

The conservation laws given by equation (12) can influence the late stages of the first-order isotropic–nematic phase transition that occurs through nucleation of nematic droplets. The droplets grow by adding molecules from the surrounding isotropic matrix and by coalescence. In early stages, the droplets are small and the director within them is practically uniform; they might form defects upon coalescence according to the Kibble mechanism, when three or more nematic droplets with different director orientation coalesce. However, as soon as the droplets grow above $R_c = K/W$, each of them acquires topological defects obeying equation (12). For the popular nematic pentylcyanobiphenyl (5CB), the surface anchoring coefficient at the nematic–isotropic interface is $W \approx 10^6\,\text{J/m}^2$ [86] while $K \approx 2 \times 10^{12}\,\text{J/m}^2$ [87]; therefore the anchoring-induced production of defects becomes effective for $R \geq R_c \approx 2\,\mu\text{m}$. Figure 6 shows nematic droplets growing from the isotropic melt (E7 mixture containing cyanobiphenyls, similar to 5CB): supramicron droplets clearly carry stable topological defects. Due to the surface anchoring that sets tilted conical director orientation (similar to 5CB, see Faetti and Palleschi [86]) there are both boojums and disclination loops [21]. As figure 6 demonstrates, the anchoring mechanism is extremely effective, producing one disclination loop per each nematic "bubble" of the appropriate size. Bowick et al. [80] expanding on the earlier studies by Chuang et al. [16], have discovered that the number of "strings" (disclinations) produced in the isotropic–nematic transition is about 0.6 per nematic "bubble" (droplet). Although this number has been found to be in reasonable agreement with the Kibble mechanism [80], it might also signal a significant contribution from the anchoring mechanism, as many droplets in the experiment [80] have been larger than $10\,\mu\text{m}$. The balance of Kibble and anchoring mechanisms in defect production during the isotropic–nematic phase transition is still an open problem. Clearly, it should strongly depend on the speed and depth
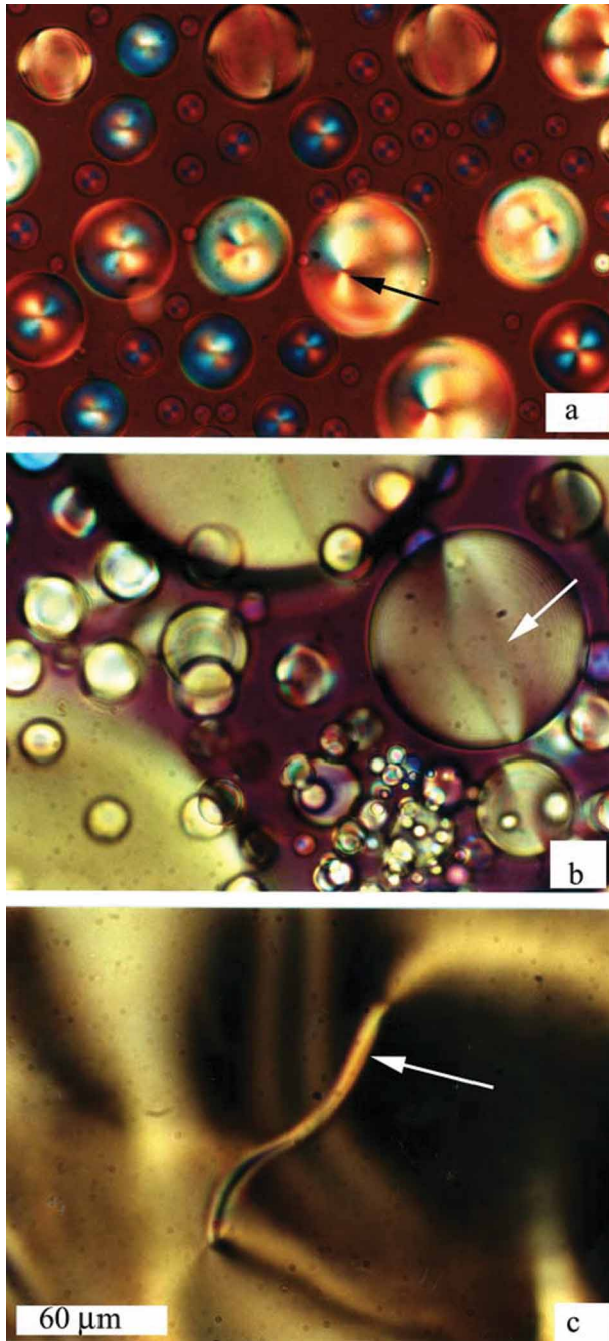
Figure 6. The sequence of textures of nematic nuclei at the isotropic–nematic transition caused by temperature quench in the mixture E7 as viewed between two crossed polarizers. The nuclei carry boojums (black arrows) and disclination loops (white arrows) (a, b); merging (c) results in disclinations with ends trapped at the cell's plates. Cell thickness $= 200\,\mu m$.

of quenching; fast quench that produces numerous submicron nuclei separated by submicron distances might avoid the anchoring mechanism. The critical radius of nucleation is $\rho_c = 2\sigma/f$ (see, for example, Kleman and Lavrentovich [4]), where $\sigma \sim 10^{-5} \mathrm{J/m^2}$ [86] is the surface tension coefficient for the isotropic–nematic interface, and f is the bulk energy density difference between the isotropic and nematic phases. Estimating $f \sim \Delta T \Delta H/T_{IN}$, where $\Delta T = T_{IN} - T$ is the depth of temperature quench and $\Delta H \sim 10^5 \mathrm{J/m^3}$ is the latent heat of transition [88], one finds the critical radius ranging from $\rho_c \sim (0.01 - 0.1)\,\mu\mathrm{m}$ when the quench is a 1–10° below T_{IN} and to $\rho_c \to \infty$ when $T \to T_{IN}$. Therefore, even a fast temperature quench might lead to large droplets if it is not deep enough. On the other hand, slow quench might tell a story of anchoring-induced defect dynamics in growing droplets that is of interest on its own, irrespective of the Kibble mechanism.

In the nematic droplets, the equilibrium director configuration and the corresponding defects change when the boundary conditions change; for example, one can cause transformations between bipolar structure with a pair of boojums and a hedgehog by changing the temperature of the sample which in its turn changes the surface orientation from tangential to normal [21, 89]. Director deformations associated with the defect structures in the droplets can cause flexoelectric polarization that contributes to electrostatic interactions between the nematic droplets [90–92].

Point defects help to stabilize nematic emulsions [93–95]. For example, imagine an isotropic (say, water) droplet with a normal boundary conditions (that can be set by adding a small amount of a surfactant such as lecithin to the system) in the nematic sample with a uniform director. If the droplet is large, then it would distort the director around itself acting as a radial hedgehog with an enlarged ''core''. If the far-field of the director is uniform, then such a droplet would create a satellite hyperbolic hedgehog that balances the topological charge $N = 1$ of the droplet. The director field around the droplet adopts a dipole configuration. When there are many droplets in the system, they attract each other at large distances and repel at distances comparable to the droplet diameter $2R$ and thus form chains of alternating droplets and hyperbolic hedgehogs. For distances $d \gg 2R$, the elastic force of attraction scales as $F \propto KR^4/d^4$ [93–95], which has been experimentally verified for the case of ferrofluid droplets [96] and most recently for solid particles manipulated by optical tweezers in the nematic bulk [75, 97].

A spectacular illustration of the role of point defects and the critical size $R_c \approx K/W$ in stabilization of emulsions has been found by Loudet *et al.* [98] who demonstrated that small isotropic oil droplets phase separating from the nematic host E7, can grow till their radius approaches $R_c \approx 2\,\mu\mathrm{m}$; after that, each oil drop forms a satellite hyperbolic hedgehog; the droplets attract each other into long chains parallel to the alignment direction of the nematic phase. Ultimately, a highly ordered array of parallel macroscopic chains is formed, made of monodisperse droplets which do not coalesce, in sharp contrast to the scenarios of phase separation in isotropic fluids. Note that the distortions around the droplets can drive them to accumulate in specific regions of the nematic matrix such as other defects (disclinations) [99] and interfaces [100, 101].

If the role of the surface anchoring is reduced (or if the electric field is applied to the droplet [102–104]), the hyperbolic hedgehog can be transformed into
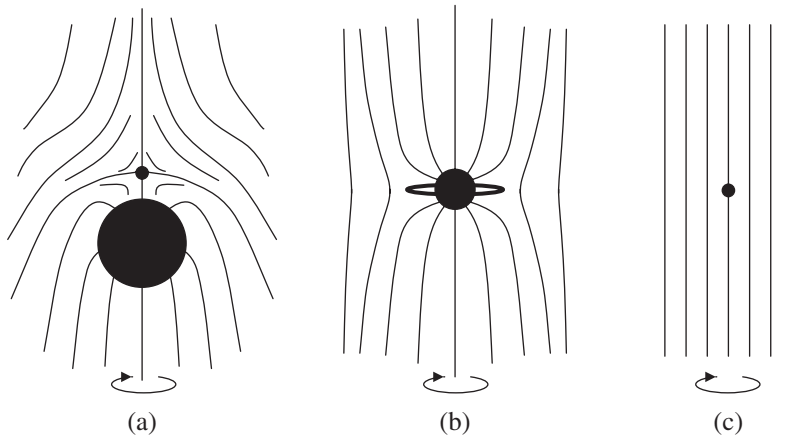
Figure 7. A spherical inclusion in a uniformly aligned nematic matrix with homeotropic boundary conditions (a) resembles a radial hedgehog and produces a hyperbolic satellite when its size is much larger than the anchoring extrapolation length K/W; (b) causes a Saturn ring configuration when the two are comparable; and (c) is ineffective to distort the director when much smaller than K/W.

an equatorial disclination loop embracing the droplet, which is known as the Saturn-ring configuration, first envisioned theoretically by Kuksenok *et al.* [105, 106] on the basis of Frank–Oseen theory; and then observed experimentally in thermotropic [107, 108] as well as lyotropic nematics [109] (figure 7). Computer simulations also suggest that the hyperbolic hedgehog can transform into the Saturn ring when the size of the spherical particle decreases [110, 111]. The interparticle interactions acquire quadrupole symmetry when the dipole hedgehog configuration changes to that of the Saturn ring symmetry in the external electric field, as demonstrated by Loudet and Poulin [104].

The interparticle interactions become much weaker, $F \propto 1/d^6$, when the normal boundary conditions are changed to the tangential ones [112, 113]. The director field acquires two defects, boojums at the poles of the particle, and the symmetry of a quadrupole. As established experimentally with the help of optical tweezers [114], the interaction might be of repulsive or attractive nature, depending on the mutual position of the two droplets, but it deviates from the quadrupolar model when the distances between the particles become comparable to a few D's.

The studies of dynamics of defect formations in colloidal systems are at the stage of infancy [115, 116]. For example, Stark and Ventzki [115] calculated the Stokes drag of spherical particles moving in a nematic host for three different configurations shown in figure 7. The hedgehog configuration is very different from the other two because of its dipolar symmetry.

4. Conclusion

The large birefringence of liquid crystals allow easy optical microscopy observations of defects, whose number is scarce in the field of view, due to the viscous relaxation

of the sample inhomogeneities; observed defects are usually in equilibrium with the boundary conditions, and of small energy. This explains why topological point defects in condensed matter physics were discovered there, in parallel with the investigations on Bloch points in magnetic bubbles [117]. This is at the origin of a noticeable (but limited) series of observations and, above all, of theoretical developments, including the topological theory of defects and their elastic and dynamic properties. The present day observation resolution is far below the advances made thanks to computational methods, in particular in the structure of the core and the anisotropy of the Frank coefficients; new experimental methods are thus awaited. One can, however, expect that more recent optical methods, such as ultra rapid confocal polarizing microscopy, attended by laser manipulations of small particles (e.g. in nematic colloidal suspensions) or even of defects themselves, might help in the investigation of macroscopic dynamic properties, at least.

Acknowledgements

References

 [1] L. Michel, Rev. Mod. Phys. **52** 617 (1980).
 [2] H. Poincaré, J. Math. **2** 151 (1886).
 [3] F.R.N. Nabarro, J. Phys., Paris **33** 1089 (1972).
 [4] M. Kleman and O.D. Lavrentovich, *Soft Matter Physics: an Introduction* (Springer, New York, 2003).
 [5] M. Kleman, O.D. Lavrentovich and Y.A. Nastishin, in *Dislocations in Solids*, edited by F.R.N Nabarro and J.P. Hirth, Vol. 12 (Elsevier, Amsterdam, 2005).
 [6] D. Hilbert and S. Cohn-Vossen, *Geometry and the Imagination* (Chelsea Publishing, New York, 1954).
 [7] M. Kleman, Phil. Mag. **27** 1057 (1973).
 [8] G.E. Volovik and V.P. Mineyev, Soviet Phys. JETP **45** 1186 (1977).
 [9] F.R.N. Nabarro, paper presented at the Conference on Fundamental Aspects of the Theory of Dislocations, Gaithersburg, April (1969). NBS Special Publi, **317**, 593 (1970).
[10] D. Melzer and F.R.N. Nabarro, Phil. Mag. **35** 901 (1977).
[11] D. Melzer and F.R.N. Nabarro, Phil. Mag. **35** 907 (1977).
[12] R.B. Meyer, Molec. Cryst. liq. Cryst. **16** 355 (1972).
[13] I. Chuang, B. Yurke, A.N. Pargellis, *et al.*, Phys. Rev. E **47** 3343 (1993).
[14] M. Hindmarsh, Phys. Rev. Lett. **75** 2502 (1995).
[15] T.W.B. Kibble, J. Phys. A **9** 1387 (1976).
[16] I. Chuang, R. Durrer, N. Turok, *et al.*, Science **251** 1336 (1991).
[17] C. Williams, P. Piéranski and P.E. Cladis, Phys. Rev. Lett. **29** 90 (1972).
[18] A. Saupe, Molec. Cryst. Liq. Cryst. **21** 211 (1973).
[19] C. Williams, P.E. Cladis and M. Kléman, Molec. Cryst. liq. Cryst. **21** 355 (1973).
[20] A. Pargellis, N. Turok and B. Yurke, Phys. Rev. Lett. **67** 1570 (1991).
[21] G.E. Volovik and O.D. Lavrentovich, Soviet Phys. JETP **58** 1159 (1983).

[22] O.D. Lavrentovich and S.S. Rozhov, Soviet Phys. JETP Lett. **47** 254 (1988).
[23] D.-K. Ding and E.L. Thomas, Molec. Cryst. liq. Cryst. **241** 103 (1994).
[24] R.B. Meyer, Phil. Mag. **27** 405 (1973).
[25] P.E. Cladis and M. Kleman, J. Phys., Paris **33** 591 (1972).
[26] S.I. Anisimov and I. Dzyaloshinskii, Soviet Phys. JETP **36** 774 (1972).
[27] G. Mazelet and M. Kleman, Polymer **27** 714 (1986).
[28] C. Chiccoli, I. Feruli, O. D. Lavrentovich, *et al.*, Phys. Rev. E **66** 030701R (2002).
[29] S. Candau and P. Le Roy Debeauvais, Molec. Cryst. liq. Cryst. **23** 283 (1973).
[30] L.A. Madsen, T.J. Dingemans, M. Nakata, *et al.*, Phys. Rev. Lett. **92** 145505 (2004).
[31] B.R. Acharya, A. Primak and S. Kumar, Phys. Rev. Lett. **92** 145506 (2004).
[32] G.E. Volovik, Soviet Phys. JETP Lett. **28** 59 (1978).
[33] M.J. Press and A.S. Arrott, J. Phys., Paris **36** C1-177 (1975).
[34] H. Brezis, J.-M. Coron and E.H. Lieb, Commun. Math. Phys. **107** 647 (1986).
[35] S. Ostlund, Phys. Rev. B **24** 485 (1981).
[36] W.F. Brinkman and P.E. Cladis, Phys. Today **35** 48 (1982).
[37] M.J. Press and A.S. Arrott, Phys. Rev. Lett. **33** 403 (1974).
[38] O.D. Lavrentovich and V.V. Sergan, Nuovo Cim. D **12** 1219 (1990).
[39] R.D. Williams, J. Phys. A **19** 3211 (1984).
[40] P. Prinsen and P. van der Schoot, J. Phys. Condensed Matter **16** 8835 (2004).
[41] F. Hélein and C.R. Hebd, Acad. Sci., Paris **305** 565 (1987).
[42] I.F. Lyuksyutov, Soviet Phys. JETP **48** 178 (1978).
[43] H. Mori and H. Nakanishi, J. Phys. Soc. Japan **57** 1281 (1988).
[44] O.D. Lavrentovich, T. Ishikawa and E.M. Terentjev, Molec. Cryst. Liq. Cryst. **299** 301 (1997).
[45] V.G. Bodnar, O.D. Lavrentovich and V.M. Pergamenschik, Soviet Phys. JETP **74** 60 (1992).
[46] J.-I. Fukuda and H. Yokoyama, Phys. Rev. E **66** 012703 (2002).
[47] N. Schopol and T.J. Sluckin, J. Phys., Paris **49** 1097 (1981).
[48] E. Penzenstadtler and H.-R. Trebin, J. Phys., Paris **50** 1027 (1981).
[49] R. Rosso and E.G. Virga, J. Phys. A **29** 4247 (1996).
[50] N. Schopol and T.J. Sluckin, Phys. Rev. Lett. **59** 2582 (1987).
[51] P. Biscari, G. Guidone Peroli and T.J. Sluckin, Molec. Cryst. Liq. Cryst. **292** 91 (1997).
[52] E.C. Gartland Jr and S. Mkaddem, Phys. Rev. E **59** 563 (1999).
[53] S. Mkaddem and E.C. Gartland Jr, Phys. Rev. E **62** 6694 (2000).
[54] S. Kralj, E.G. Virga and S. Zumer, Phys. Rev. E **60** 1858 (1999).
[55] S. Kralj and E.G. Virga, J. Phys. A **34** 829 (2001).
[56] O.D. Lavrentovich, P. Pasini, C. Zannoni, *et al.* (Editors), *Defects in Liquid Crystals: Computer Simulations, Theory and Experiment* (Kluwer Academic, Dordrecht, The Netherlands, 2001).
[57] A.N. Semenov, Europhys. Lett. **46** 631 (1999).
[58] E.C. Gartland Jr, A.M. Sonnet and E.G. Virga, Continuum Mech. Thermodyn. **14** 307 (2002).
[59] G. Guidone Peroli and E.G. Virga, Phys. Rev. E **54** 5235 (1996).
[60] G. Guidone Peroli and E.G. Virga, Phys. Rev. E **56** 1819 (1997).
[61] I. Vilfan, M. Vilfan and S. Zumer, Phys. Rev. A **43** 6875 (1991).
[62] G.P. Crawford, M. Vilfan, J.W. Doane, *et al.*, Phys. Rev. A **34** 835 (1991).
[63] Z. Bradac, S. Kralj and S. Zumer, Phys. Rev. E **58** 7447 (1998).
[64] R. Holyst and P. Oswald, Phys. Rev. E **65** 041711 (2002).
[65] L.M. Pismen and B.Y. Rubinstein, Phys. Rev. Lett. **69** 96 (1992).
[66] Y.A. Dreizen and A.M. Dykhne, Sov. Phys. JETP **34** 1140 (1972).

[67] K. Minoura, Y. Kimura, K. Ito, *et al.*, Phys. Rev. E **58** 643 (1998).
[68] A.N. Pargelis, P. Finn, J.W. Goodby, *et al.*, Phys. Rev. A **46** 7765 (1992).
[69] D.R. Link, M. Nakata, K. Ishikawa, *et al.*, Phys. Rev. Lett. **87** 195507 (2001).
[70] P.E. Cladis and H.R. Brand, Physica A **326** 322 (2003).
[71] G. Guidone Peroli, G. Hilling, A. Saupe, *et al.*, Phys. Rev. E **58** 3259 (1998).
[72] M. Svetec, Z. Bradac, S. Krali, *et al.*, Molec. Cryst. Liq. Cryst. **413** 43 (2004).
[73] A. Zywocinski, K. Pawlak, R. Holyst, *et al.*, J. Phys. Chem. B **109** 9712 (2005).
[74] J.-I. Hotta, K. Sasaki and H. Masuhara, Appl. Phys. Lett. **71** 2085 (1997).
[75] I.I. Smalyukh, A.N. Kuzmin, A.V. Kachynski, *et al.*, Appl. Phys. Lett. **86** 021913 (2005).
[76] C. Blanc, D. Svensek, S. Zumer, *et al.*, Phys. Rev. Lett. **95** 097802 (2005).
[77] H. Arodz, J. Dziarmaga, W.H. Zurek (Editors), *Patterns of Symmetry Breaking* (Kluwer Academic, Dordrecht, The Netherlands, 2003).
[78] H. Toyoki, Phys. Rev. A **42** 911 (1990).
[79] R.A. Wickham, Phys. Rev. E **56** 6843 (1997).
[80] M.J. Bowick, L. Chandar, E.A. Schiff, *et al.*, Science **263** 943 (1994).
[81] A.N. Pargellis, J. Mendez, M. Srinivasarao, *et al.*, Phys. Rev. E **53** R25 (1996).
[82] I. Dierking, O. Marshall, J. Wright, *et al.*, Phys. Rev. E **71** 061709 (2005).
[83] P.S. Drzaic, *Liquid Crystal Dispersion* (World Scientific, Singapore, 1995).
[84] H. Stark, Phys. Rep. **351** 387 (2001).
[85] P. Poulin, Curr. Opin. Colloid Interface Sci. **4** 66 (1999).
[86] S. Faetti and V. Palleschi, Phys. Rev. A **30** 3241 (1984).
[87] M.J. Bradshaw, E.P. Raynes, J.D. Bunning, *et al.*, J. Phys., Paris **46** 1513 (1985).
[88] H. Yokoyama, J. Chem. Soc. Faraday Trans. **2** 84 (1988).
[89] O.O. Prishchepa, A.V. Shabanov and V.Y. Zyryanov, Phys. Rev. E **72** 031712 (2005).
[90] R.B. Meyer, Phys. Rev. Lett. **22** 918 (1969).
[91] O.D. Lavrentovich, Soviet Tech. Phys. Lett. **14** 73 (1988).
[92] N.M. Golovataya, M.V. Kurik and O.D. Lavrentovich, Liq. Cryst. **7** 287 (1990).
[93] P. Poulin, H. Stark, T.C. Lubensky, *et al.*, Science **275** 1770 (1997).
[94] T.C. Lubensky, D. Pettey, N. Currier, *et al.*, Phys. Rev. E **57** 610 (1998).
[95] P. Poulin and D.A. Weitz, Phys. Rev. E **57** 626 (1998).
[96] P. Poulin, V. Cabuil and D.A. Weitz, Phys. Rev. Lett. **79** 4862 (1997).
[97] M. Yada, J. Yamamoto and H. Yokohama, Phys. Rev. Lett. **92** 185501 (2004).
[98] J.-C. Loudet, P. Barois and P. Poulin, Nature **407** 611 (2000).
[99] D. Voloschenko, O.P. Pishnyak, S.V. Shiyanovskii, *et al.*, Phys. Rev. E **65** 060701R (2002).
[100] J.L. West, K. Zhang, A.V. Glushchenko, *et al.*, Molec. Cryst. Liq. Cryst. **422** 73 (2004).
[101] M. Mitov, F. De Guerville and C. Bourgerette, Molec. Cryst. Liq. Cryst. **435** 673 (2004).
[102] H. Stark, Eur. Phys. J. B **10** 311 (1999).
[103] H. Stark, Phys. Rev. E **66** 032701 (2002).
[104] J.C. Loudet and P. Poulin, Phys. Rev. Lett. **87** 165503 (2001).
[105] O.V. Kuksenok, R.W. Ruhwandl, S.V. Shiyanovskii, *et al.*, Phys. Rev. E **54** 5198 (1996).
[106] S.V. Shiyanovskii and O.V. Kuksenok, Molec. Cryst. Liq. Cryst. A **321** 489 (1998).
[107] Y. Gu and N.L. Abbott, Phys. Rev. Lett. **85** 4719 (2000).
[108] J.C. Loudet, O. Mondain-Monval and P. Poulin, Eur. Phys. J. E **7** 205 (2002).
[109] O. Mondain-Monval, J.C. Dedieu, T. Gulik-Krzywicki, *et al.*, Eur. Phys. J. B **12** 167 (1999).
[110] A.-I. Fukuda, M. Yoneya and H. Yokoyama, Phys. Rev. E **65** 041709 (2002).
[111] D. Andrienko, G. Germano and M.P. Allen, Phys. Rev. E **63** 041701 (2001).
[112] S. Ramaswamy, R. Nityananda, V. Raghunathan, *et al.*, Molec. Cryst. Liq. Cryst. **228** 175 (1996).

[113] R.W. Ruhwandl and E.M. Terentjev, Phys. Rev. E **55** 2958 (1997).

[114] I.I. Smalyukh, O.D. Lavrentovich, A.N. Kuzmin, *et al.*, Phys. Rev. Lett. **95** 157801 (2005).

[115] H. Stark and D. Ventzki, Phys. Rev. E **64** 031711 (2001).

[116] J.-I. Fukuda, H. Stark and H. Yokoyama, Phys. Rev. E **72** 021701 (2005).

[117] A.P. Malozemoff and J.C. Slonczewski, *Magnetic Domain Walls in Bubble Materials* (Academic Press, New York, 1979).